

Constraints on the mass of a bosonic dark matter candidate within the DD2Y-T model

Mahboubeh Shahrbafe^{1,2,*} , Davood Rafiei Karkevandi^{3,4}  and Stefan Typel^{5,6} 

- ¹ Incubator of Scientific Excellence—Centre for Simulations of Superdense Fluids, University of Wrocław; m.shahrbafe46@gmail.com
- ² Frankfurt Institute for Advanced Studies, Giersch Science Center, D-60438 Frankfurt am Main, Germany; motlagh@fias.uni-frankfurt.de
- ³ Department of Physics, Isfahan University of Technology, Isfahan 84156-83111, Iran; davood.rafiee64@gmail.com
- ⁴ ICRANet-Isfahan, Isfahan University of Technology, 84156-83111, Iran; davood.rafiee64@gmail.com
- ⁵ Technische Universität Darmstadt, Fachbereich Physik, Institut für Kernphysik, Schlossgartenstraße 9, D-64289 Darmstadt, Germany; stypel@ikp.tu-darmstadt.de
- ⁶ GSI Helmholtzzentrum für Schwerionenforschung GmbH, Theorie, Planckstraße 1, D-64291 Darmstadt, Germany
- * Correspondence: motlagh@fias.uni-frankfurt.de
- † Present address: Frankfurt Institute for Advanced Studies, Giersch Science Center, D-60438 Frankfurt am Main, Germany

Abstract: Dark matter remains a topic of ongoing controversy. It has gained attention in the theoretical description of compact objects such as neutron stars with cores of very dense matter. Various candidates have been proposed for dark matter in the scientific literature. Among them, the sexaquark has been identified as a potential bosonic particle capable of being formed in neutron star matter based on its mass characteristics. In this study, we investigate the viability of the sexaquark as a candidate for dark matter, particularly under certain density conditions. Our goal is to address the challenges associated with the formation of a bosonic particle in a highly dense medium without compromising the stability of the neutron star. To achieve this, we introduce a straightforward linear mass shift for the sexaquark within the hadronic equation of state, utilizing a relativistic density functional approach. In our investigation, it is observed that the inclusion of Sexaquark as a candidate for dark matter within the hadronic matter equation of state, although featuring a repulsive interaction with baryonic matter, softens the equation of state. We suppose that the strength of the interaction of dark matter with baryonic matter increases linearly with the baryon density. We observe that raising the effective mass of the Sexaquark, as a result of increasing its vacuum mass, causes an increased stiffening of the equation of state as compared to the case of a constant mass. We determine the lower and upper mass boundaries for this bosonic dark matter based on observational constraints for neutron stars within the DD2Y-T model when a phase transition to quark matter phase is employed.

Keywords: Dark matter, Neutron star, Equation of State, Relativistic Mean-Field, Phase transition, Sexaquark

Citation: Shahrbafe, M.; Rafiei Karkevandi, D.; Typel, S. Constraints on the mass of bosonic dark matter candidate within DD2Y-T model. *Journal Not Specified* **2023**, *1*, 0. <https://doi.org/>

Received:

Revised:

Accepted:

Published:

Copyright: © 2024 by the authors. Submitted to *Journal Not Specified* for possible open access publication under the terms and conditions of the Creative Commons Attribution (CC BY) license (<https://creativecommons.org/licenses/by/4.0/>).

1. Introduction

The accepted cosmological models that are presented and founded in General Relativity (GR), suggest that almost 27% of the matter-energy composition of the universe exists in the form of enigmatic Dark Matter (DM) [1].

Multi-messenger astrophysics is actively engaged in the search for and examination of new ideas concerning dark-matter particles. These candidates are believed to be non-relativistic particles that exist beyond the Standard Model of particle physics. They interact weakly with ordinary baryonic matter solely through gravitational forces [2]. In this context, the most widely accepted candidates for DM are weakly interacting massive

particles (WIMPs) [3,4]. However, hypothetical bosonic particles such as the axion [5,6] and the sexaquark [7,8] also exhibit the primary characteristics required to be considered as potential DM candidates. Their interaction with the baryonic matter must be very weak, which is why they have remained undetected thus far.

A broad spectrum for the mass of candidates for DM particles exists, spanning a wide range from approximately 10^{-22} eV to 10^{10} eV, contingent on the particular type of candidate. DM particles must be incorporated into an equation of state (EoS), which is a fundamental tool for characterizing matter, whereas the EoS for strongly interacting matter in neutron stars (NSs) is tightly bound by observational constraints. Therefore, efficient constraints on the features of DM candidates have been established using recent advancements in observational astronomy [9–15], mainly facilitated by gravitational wave (GW) interferometers and the Neutron Star Interior Composition Explorer (NICER). One can refer to the works [16–18] and the references therein as illustrative examples of how the properties of DM can be constrained through multi-messenger observations of neutron stars. It is worth mentioning that Compact objects, such as white dwarfs, NSs, and strange stars, have the potential to include DM particles due to their high baryonic density. In particular, NSs are one of the well-known astrophysical laboratories for investigating DM because they are the densest environment known in the universe so far, except for black holes. Therefore, various studies have investigated the inclusion of either bosonic or fermionic DM candidates in NSs using different approaches [19–33].

The concept of a deeply bound Sexaquark (S), an alternative term for the hexaquark family of hypothetical particles, was first introduced as a bosonic candidate for DM in references [7,8,34]. The quark composition of S is identical to that of the H-dibaryon [35], with both consisting of uuddss quarks. However, S exhibits significantly stronger binding compared to the H-dibaryon. If S represents a molecular state like $\Lambda\Lambda$, it is important to note that Λ is characterized as a color-neutral particle. In this context, the binding of two Λ particles can exclusively occur through the exchange of color-neutral entities, such as mesons. When S comprises a complex system consisting of three colored diquarks, it becomes essential to acknowledge that these entities engage in interactions primarily governed by the color force. This force is notably more potent than the meson exchange force, particularly when considering short-range distances.

The proposed S is a boson at a spin-color-flavor singlet and even parity state, characterized by a zero electric charge, a baryon number of 2, and a strangeness value of -2. S may manifest itself as a deeply bound state, displaying a mass sufficiently low to render it either absolutely or effectively stable against decay. The potential of S to serve as DM hinges on its mass and its propensity to dissociate into two baryons, emphasizing the need for a small dissociation amplitude. An S particle lighter than deuterium cannot decay without violating baryon number conservation and, consequently, remains stable. This condition is met when the mass of S is less than the sum of the proton mass, electron mass, and Lambda baryon mass, which totals 2054.46 MeV — the lowest mass value consistent with a $\Delta S = 1$ decay. Moreover, the ratio of densities between S dark matter and ordinary baryonic matter in the Universe that can be estimated through considerations of statistical equilibrium within the quark-gluon plasma, utilizing known parameters from Quantum Chromodynamics (QCD), aligns with observational data. Under such conditions, S emerges as a viable DM candidate [7]. A scheme in which such a state could be produced at rest through the formation of anti-protonic atoms has been proposed in [8].

In our prior work [36], referred to as ‘paper I’ hereafter, we established the lower-mass limit for S using a generalized relativistic density functional (GRDF) approach known as DD2Y-T, ensuring that the possible emergence of S as a DM candidate remains consistent with observational constraints derived from NS. Our findings disclosed the feasibility of S appearance in the hadronic phase of NS, demonstrating that a minimum mass of $m_S = 1885$ MeV fulfills the necessary conditions that S does not appear at subsaturation densities. The stability of such stars is contingent on both a positive mass shift for S and a phase transition into deconfined quark matter. In this present study, we adopt the same approach

to ascertain the upper limit for the mass of S . We aim to investigate whether S remains a viable stable bosonic DM candidate across the entire accepted mass range within our model.

The paper is organized as follows: In Section 2, we present the EoS for hadronic matter including DM within the framework of the GDRF model with density-dependent couplings applied to NS matter. In Section 3, we introduce the EoS for quark matter. The hybrid EoS employing a cross-over transition is derived in section 4. Our findings and in-depth discussions concerning the properties of the resulting hybrid stars, as well as the mass of S , are presented in Section 5. Finally, we summarize our work and draw conclusions in Section 6.

2. Hadronic Matter Equation of State Including Dark Matter

The hadronic phase of matter is postulated to encompass all nucleons and hyperons, namely the neutron, proton, Λ , Σ , Ξ , and our DM candidate ' S '. These baryons are analyzed within the core of NS using a GRDF approach. In this approach, all particles are treated as quasi-particles with effective mass and effective chemical potential. The interactions in this model exclusively entail meson exchange interactions, and the couplings to these mesons depend on the density of the medium. The density-dependent couplings are meticulously adjusted to faithfully reproduce the characteristics of atomic nuclei, as established by earlier works [37–39].

For our investigation, we have employed an extended EoS, denoted as DD2Y-T, which accounts for all octet baryons. The interaction is described by the exchange of σ , ω , ρ , and ϕ mesons. This EoS has been employed to assess the properties of NSs in both high-temperature, or "hot", and low-temperature, or "cold", hyperonic configurations [40]. Notably, it is essential to highlight that this model successfully addresses the 'hyperon puzzle', a conundrum that has been extensively deliberated in the literature and is considered one of the most challenging issues within the domain of hypernuclear physics [41–44].

In the DD2Y-T_S model, the S particle serves as an additional baryonic degree of freedom, featuring a mass shift that depends on the baryonic density, which captures the impact of its interaction with the surrounding medium. In principle, the interaction between the S particle and the surrounding medium can be theoretically elucidated by establishing couplings to mesons, akin to the approach employed for other baryonic degrees of freedom. However, this endeavor necessitates the introduction of several meson-sexaquark couplings, the precise values of which remain undetermined.

As established in paper I [36], we have demonstrated that a constant mass assumption for the S particle is incompatible with the structural stability of NS. Consequently, we introduced a linear density-dependent mass shift for the S particle, with a slope parameter harmonized with the corresponding mass shifts observed in other baryons. Detailed constraints regarding the lower threshold of the mass and the slope parameter have been thoughtfully presented and illustrated in Figure 8 of paper I. In our approach

$$S_S = -\Delta m_S, \quad (1)$$

is the scalar potential for the S particle and Δm_S is the mass shift of S . The effective mass for S is thus defined as

$$m_S^* = m_S - S_S = m_S + \Delta m_S, \quad (2)$$

with the vacuum mass m_S of S . The mass shift is given by

$$\Delta m_S = m_S x_S \frac{n_b}{n_0}. \quad (3)$$

where n_b is the baryonic density, x_S is a slope parameter and $n_0 = 0.15 \text{ fm}^{-3}$ is the nuclear saturation density. A finite density of S exclusively emerges at zero temperature when the

condition $m_S^* = \mu_S^*$ is met, leading to the occurrence of Bose-Einstein condensation. The scalar density for S then is equal to the vector density and reads

$$n_S^{(s)} = n_S^{(v)} = n_b - n_n^{(v)} - n_p^{(v)} - n_\Lambda^{(v)} - n_{\Sigma^+}^{(v)} - n_{\Sigma^0}^{(v)} - n_{\Sigma^-}^{(v)} - n_{\Xi^0}^{(v)} - n_{\Xi^-}^{(v)}. \quad (4)$$

Here, $n_i^{(v)}$ signifies the vector density of the fermions. All relevant information pertaining to the thermodynamic properties of the system can be deduced from the grand canonical thermodynamic potential density, denoted as $\Omega(\mu_i)$, wherein μ_i signifies the chemical potential of each particle at zero temperature. The condensate contribution of the bosonic S in grand canonical thermodynamic potential is formally given by

$$\Omega_S = n_S^{(s)}(m_S^* - \mu_S^*), \quad (5)$$

where $\mu_S^* = \mu_S - V_S$ is the effective potential and $\mu_S = 2\mu_b$ is the chemical potential of S particle. V_S is the vector potential for the S particle and reads

$$V_S = n_S^{(s)} \frac{\partial \Delta m_S}{\partial n_S^{(v)}}. \quad (6)$$

It appears as rearrangement contribution due to the density dependence of the mass shift and is required for thermodynamic consistency. For a more comprehensive exploration of the topic, we refer the reader to the extensive discussion presented in paper I.

The pressure (P) can be straightforwardly expressed as $P = -\Omega$. Moreover, the free energy density (f) coincides with the internal energy density (ε) and can be readily computed using the following relation:

$$f = \varepsilon = \Omega + \sum_i \mu_i n_i^{(v)}. \quad (7)$$

3. Quark-matter Equation of State

One of the best candidates for describing the color superconducting quark matter phase is a covariant nonlocal Nambu–Jona–Lasinio (nlNJL) model [45]. This effective model successfully accounts for the key features of low-energy QCD, such as dynamical chiral symmetry breaking, and also reasonably fulfills NS conditions.

In this effective model, it is worth noting that the precise values of the vector meson coupling and the diquark coupling remain undetermined. In one study, we have determined optimal parameters for those couplings in the nlNJL model [46]. This was achieved through Bayesian analysis, specifically in the context of a first-order phase transition from hadronic matter to deconfined quark matter within a systematic study of hybrid neutron star EoS.

In this study, we have utilized the selected parameters from reference [46] to establish a phase transition from the DD2Y-T_S model to the nlNJL model. The chosen parameters fall within the range of $0.10 < \eta_V < 0.12$ and $0.70 < \eta_D < 0.74$. As mentioned, these parameter selections were made through Bayesian analysis, considering the contemporary mass and radius constraints of NSs. For the Bayesian analysis in reference [46], two constraints derived from observations of neutron stars have been employed. The first constraint is based on the mass-radius measurements of the neutron star component within the binary system PSR J0740+6620, determined using the relativistic Shapiro time delay effect. The gravitational mass of this neutron star is estimated to be approximately $2.08_{-0.07}^{+0.07} M_\odot$ with a 68% credibility interval, as reported in references [14]. The neutron star's radius has been inferred through fitting rotating hot spot patterns to data from the Neutron Star Interior Composition Explorer (NICER) and X-ray Multi-Mirror (XMM-Newton) X-ray observations, resulting in an estimated radius of approximately $13.7_{-1.5}^{+2.6}$ km at the 68% confidence level, as reported in reference [11]. The second constraint utilized in our analysis pertains to the radius of a neutron star with a mass of $1.4 M_\odot$, estimated to be approximately $11.75_{-0.81}^{+0.86}$

km at a 90% confidence level. This constraint was derived through a combined analysis of the gravitational-wave event GW170817 with its electromagnetic counterparts AT2017gfo and GRB170817A, as well as the gravitational-wave event GW190425, both originating from neutron-star mergers, as described in reference [15].

4. Hybrid Equation of State

This study utilizes a crossover construction, often referred to as a mixed-phase approach, to model the phase transition between the hadronic and quark phases [44]. The hadronic equation of state (EoS) is considered appropriate at lower densities, particularly in the vicinity of nuclear saturation density, where the baryonic matter does not reveal its mixed structure. We establish the upper limit of applicability for our hadronic EoS as $n_H(\mu)$. In regions of relatively high densities, where quarks exist independently of specific baryons, the deconfined quark matter EoS is invoked. The lower threshold of validity for the color superconducting quark matter EoS is defined as $n_Q(\mu)$. In the intermediate density range, denoted by $n_H(\mu) < n(\mu) < n_Q(\mu)$, neither the hadronic EoS nor the quark matter EoS is suitable.

The determination of surface tension at the interface between the hadronic phase and quark phase in strongly interacting matter remains a topic of ongoing investigations. An infinite surface tension implies the applicability of a Maxwell construction, whereas a vanishing surface tension necessitates the use of a Glendenning construction. In scenarios where the surface tension is variable, a cross-over construction approach can be considered.

As the EoS for the hadronic and quark matter phases are expressed in terms of the relationship between pressure and chemical potential, denoted as $P_H(\mu)$ and $P_Q(\mu)$, respectively, specifically at $T = 0$ conditions relevant for NS, the effective cross-over EoS $P_M(\mu)$ can be conveniently represented as an interpolation function between these two phases. This interpolation requires that the pressure function seamlessly connects the values characteristic of hadronic and quark phases at their lower and upper limits. Moreover, it must satisfy fundamental thermodynamic constraints, including a positive slope of density versus chemical potential, i.e., $\frac{\partial n_M}{\partial \mu_M} = \frac{\partial^2 P_M}{\partial \mu_M^2} > 0$. Additionally, the causality condition, which ensures that the adiabatic speed of sound at zero frequency, $c_s^2 = \frac{\partial P}{\partial \epsilon}$, does not exceed the speed of light, must be adhered to. One effective and practical approach for achieving this interpolation is through the utilization of a polynomial function, which smoothly connects the pressure curves of the two phases.

The critical chemical potential, denoted as μ_c , defines the point at which two phases achieve both mechanical and chemical equilibrium. It is determined through the Maxwell point, encompassing both the physical transition and a non-physical transition referred to as reconfinement, expressed as:

$$P_Q(\mu_c) = P_H(\mu_c) = P_c. \quad (8)$$

To model the pressure of the cross-over phase, we employ a polynomial ansatz:

$$P_M(\mu) = \sum_{q=1}^N \alpha_q (\mu - \mu_c)^q + (1 + \Delta_P) P_c. \quad (9)$$

Here, Δ_P represents a free parameter that characterizes the pressure of the cross-over phase at μ_c :

$$P_M(\mu_c) = P_c + \Delta_P = P_M, \text{ where } \Delta_P = \frac{\Delta P}{P_c}. \quad (10)$$

The value of Δ_P is intricately related to the surface tension existing at the interface between the two phases. Typically, within the framework of equation (9), it is common to consider $N = 2$.

At the matching points μ_H and μ_Q , the pressure of the cross-over phase aligns with the pressure of the hadronic and quark matter phases, respectively. This requires that both pressures and their first derivatives satisfy continuity conditions, as outlined below:

$$P_H(\mu_H) = P_M(\mu_H), \quad (11)$$

$$P_Q(\mu_Q) = P_M(\mu_Q), \quad (12)$$

$$\frac{\partial}{\partial \mu} P_H(\mu_H) = \frac{\partial}{\partial \mu} P_M(\mu_H), \quad (13)$$

$$\frac{\partial}{\partial \mu} P_Q(\mu_Q) = \frac{\partial}{\partial \mu} P_M(\mu_Q). \quad (14)$$

By considering the relationship $n(\mu) = \frac{\partial P(\mu)}{\partial \mu}$, we undertake a numerical solution of the continuity equations, i.e., (11-14) for baryon density. This approach enables us to deduce the unknown variables in the aforementioned equations.

It is notable to emphasize that for the employed EoSs, the first crossing between the hadronic phase and the deconfined quark matter phase takes place at extremely low densities. Consequently, we employ a cross-over construction for the second crossing corresponding to the reconfinement transition from the quark phase to the hadronic phase at higher densities, wherein $\Delta p < 0$. This approach allows the hadronic equation of state to remain applicable at lower densities, while the quark matter equation of state remains valid at higher densities.

5. Results

In paper I, specific values for the slope parameter, denoted as x_S which is in accordance with the coupling strength, and the vacuum mass of S m_S in equation (3) were carefully chosen to satisfy the constraints arising from the interplay of these two parameters. The graphical representation of these constraints, depicting x_S as a function of m_S is illustrated in Figure 8 of Paper I. It is noteworthy that the DD2Y-T model, characterized by parameters fine-tuned to the properties of atomic nuclei around saturation density, offers an extrapolation of the EoS beyond the saturation point, rendering it less stringently constrained at high densities.

Consequently, the constraints derived from the saturation properties, as delineated in Figure 8 of Paper I, are notably more robust. Specifically, the lower boundaries for the mass and the coupling strength pertaining to S particles are established from the yellow and pink lines, yielding values of $m_S^{\min} = 1885$ MeV and $x_S^{\min} = 0.03$ respectively. Conversely, other constraints are based on the observations of NSs at high densities and may exhibit a degree of model dependency. Consequently, the forthcoming work will focus on investigating the model-dependent aspects of the current results.

This study aims to explore the upper limit for the mass of S as a candidate for DM within the framework of the DD2Y-T model. To ascertain the permissible range for the mass of S , it is important to venture into high-density regimes and ensure the alignment of outcomes with observational constraints associated with NSs. It is essential to note that a mass shift of S particles, x_S , serves the purpose of mimicking the interaction with the surrounding medium. Given the postulation that S is a candidate for DM, it is reasonable to anticipate a predominantly weak interaction with the medium. Consequently, even though elevating the mass of S would inherently enable us to increase the value of x_S based on Figure 8 in paper I, it is a deliberate choice to maintain x_S as the coupling strength of the DM interaction with baryonic matter at its minimal value, specifically $x_S = 0.03$ throughout the subsequent analyses.

It is imperative to note that in the lower panels of Figure 9 in Paper I, increasing the value of x_S results in the outward displacement of the Mass-Radius (M-R) curve towards the outer region of the green band surrounding $1.4M_\odot$ which represents a crucial observational constraint relating to the mass and radius of NSs. This choice allows us to play with the

value of the vacuum (and consequently effective) mass of the DM candidate and investigate its role in the consistency of the EoS of the hybrid star with the observables.

We take the successful procedure of paper I and investigate it for the higher vacuum masses of S . Therefore, we employ the replacement interpolation construction (RIC) based on what was explained in Section 4 for a phase transition from hadronic matter to deconfined quark matter.

Figure 1 illustrates the pressure as a function of the baryonic chemical potential, showcasing both the hadronic phase and the quark phase. In the context of the hadronic phase, the coupling strength of S remains constant, as previously discussed, while different values of the vacuum mass of S are supposed but the effective mass exhibits an increasing trend. One should notice that in comparison to the hadronic EoS without S (as represented by DD2Y-T, which includes nucleons and hyperons), the inclusion of S as a DM candidate results in an obvious softening of the EoS, although a repulsive interaction between DM and baryonic matter is considered. In the quark phase, we depict various EoSs with specific parameters determined through Bayesian analysis, as outlined in reference [46]. These EoSs are characterized by three key parameters: the diquark coupling (η_D), the vector meson coupling (η_V), and the square of the speed of sound ($c_s^2 = \frac{dP}{d\varepsilon}$), which serves as an indicator of EoS stiffness.

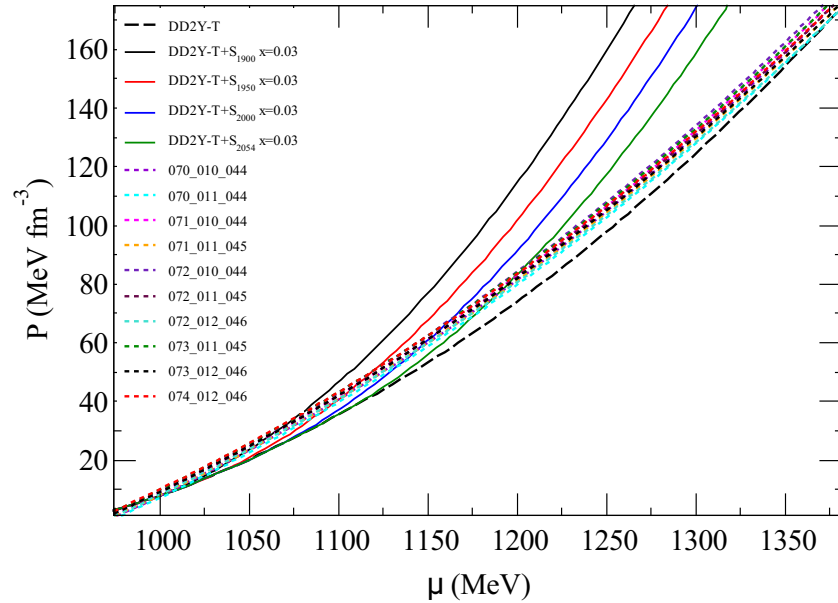


Figure 1. Pressure as a function of baryonic chemical potential for both hadronic phase and quark phase. The solid lines correspond to the hadronic phase with S for which the coupling strength of S remains constant while different values of the vacuum mass of S are supposed. The quark matter EoSs shown with dotted lines are characterized by three key parameters: the diquark coupling (η_D), the vector meson coupling (η_V), and the square of the speed of sound, respectively. The hadronic EoS without S is also shown with the black dashed line as DD2Y-T for comparison.

Figure 2 visually distinguishes and presents the low chemical potential region and the high chemical potential region, distinctly depicted in the left and right panels, respectively.

The purpose of presenting these two regions separately is twofold. Firstly, it serves to elucidate the physical transition from the hadronic phase to the quark phase in the left panel, which transpires at exceptionally low chemical potentials, near saturation density, where the emergence of deconfined quark matter or even S particles is not anticipated. Secondly, the high chemical potential region in the right panel reveals the reconfinement

point, where the RIC has been applied to correct the mischaracterization of the transition. As a result, at lower densities, the hadronic phase prevails, while at high densities, the quark phase remains a valid description. It is noteworthy that, for each hadronic EoS, we have chosen the initial intersection point with the quark phase lines in the right panel to serve as the basis for implementing the phase transition construction. But one aspect to highlight is that all the quark matter lines with favorable parameters as derived in [46] are applicable to the present investigation.

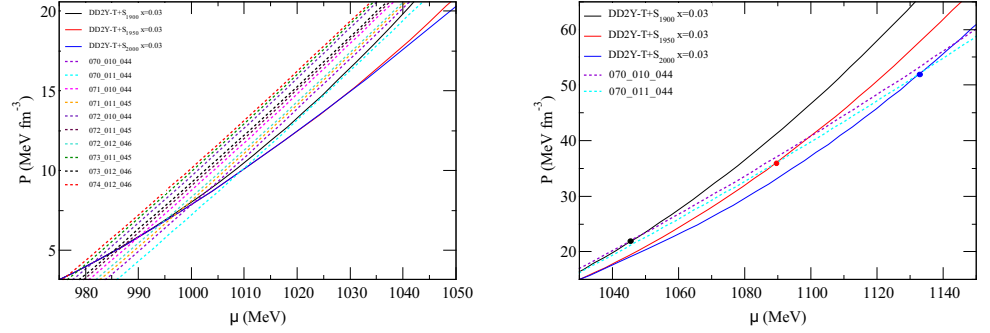


Figure 2. Same as Figure 1. The left panel shows the low chemical potential region while the right panel corresponds to the high chemical potential region. The dots on the right panel show the critical chemical potential in Eq. (8) at which the RIC has been applied.

It is worth noticing in the right panel of Figure 2, when x_S is held constant as a representative of the coupling strength of S interaction with the medium, increasing the vacuum mass of S particles (resulting in an increased effective mass of S) leads to a stiffening of the EoS, subsequently shifting the reconfinement onset to higher densities. As a result, a higher fraction of S particles as DM candidates will be produced in the stellar matter. A more detailed discussion regarding the fraction of DM within our model and our scenario is a topic for our future research.

Ultimately, Figure 3 delineates the distinct intersection points where the hadronic phase intersects with the quark matter phase, each accompanied by their respective hybrid EoS as obtained within the framework of RIC. The matching points defined earlier as μ_H and μ_Q , represent the chemical potentials at which the pressure of the crossover phase is in concordance with the pressures of the hadronic and quark matter phases, clearly illustrated across the three panels.

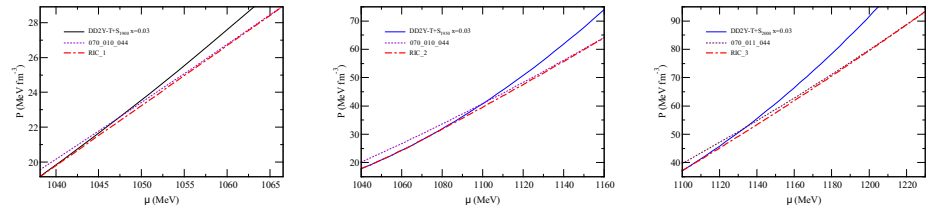


Figure 3. Pressure as a function of baryonic chemical potential for the hadronic phase, quark matter phase, and the hybrid EoS constructed within the framework of RIC for all three points shown in the right panel of Figure 2

It is clearly illustrated in Figure 3 how a negative value for Δp in the context of RIC effectively addresses the issue of a nonphysical intersection point, often referred to as the reconfinement point. This adjustment restores the hadronic phase at lower densities and the quark matter phase at higher densities.

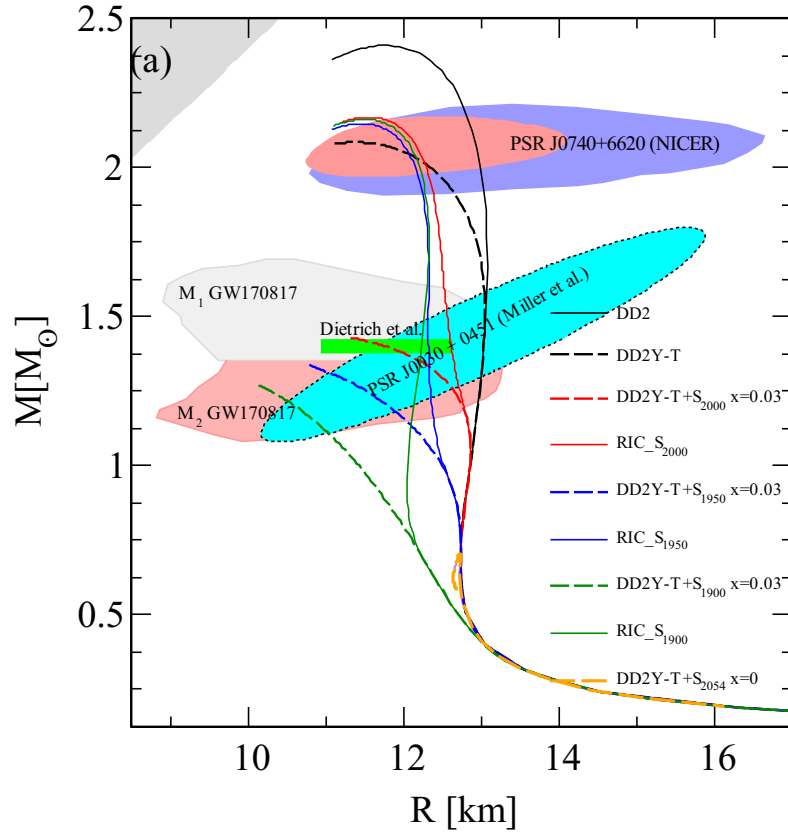


Figure 4. Mass-Radius curves for compact stars with a pure nucleonic core (black solid line), hypernucleonic core (black dashed line), hadronic core with S (dashed colorful lines), and hybrid stars with a quark matter core (solid colorful lines). For a comparison the new $1 - \sigma$ mass-radius constraints from the NICER analysis of observations of the massive pulsar PSR J0740+6620 [14] are indicated in red [13] and blue [11] regions. Additionally, the green bar marks the radius of a $1.4 M_{\odot}$ neutron star from a joint analysis of the gravitational-wave signal GW170817 with its electromagnetic counterparts at 90% confidence [15].

5.1. Discussion based on the observational constraints of neutron stars

At the present time, the only way we can assess the accuracy of our hybrid solutions is by comparing them to observations of dense compact stars at high densities. To this end, both pure hadronic EoSs and hybrid ones are incorporated as inputs into the Tolman-Oppenheimer-Volkoff (TOV) equations, yielding the M-R diagram for each EoS. It is worth noting that the standard unified DD2 EoS, which also accounts for the crust of compact stars, has been utilized. The outcomes are presented graphically in Figure 4. The observational constraints are represented by color-coded regions in this figure.

In Figure 4, it is evident that none of the pure hadronic EoSs can simultaneously satisfy all imposed constraints. In contrast, all hybrid EoSs are successfully in favor of these constraints and this should be attributed to including DM in the hadronic phase. Notably, the figure illustrates the considerable trend in M-R curves as they pass the boundary defined by the green bar, which signifies the constraint on the radius of $1.4 M_{\odot}$ stars. This behavior is attributed to the increased mass of S particles, which enhances the stiffness of the EoS and consequently results in larger stellar radii. Specifically, the red curve, corresponding to $m_S = 2000$ MeV, passes the border of the green bar. Therefore, we establish this mass value as the upper limit for the vacuum mass of S particles.

Furthermore, the recent detection of gravitational-wave (GW) signals arising from binary NS mergers, along with the subsequent determination of the tidal deformability parameter, have opened a new window for investigating the exotic internal structures of NSs [47,48]. Tidal deformability, which characterizes the susceptibility of a NS to deformation within a binary system, is exceptionally sensitive to the EoS governing NS matter and its compactness [49,50]. Consequently, we analyze the consistency of our model with respect to the tidal deformability constraint for a ($1.4M_{\odot}$) NS, $\Lambda_{1.4} = 190^{+390}_{-120}$.

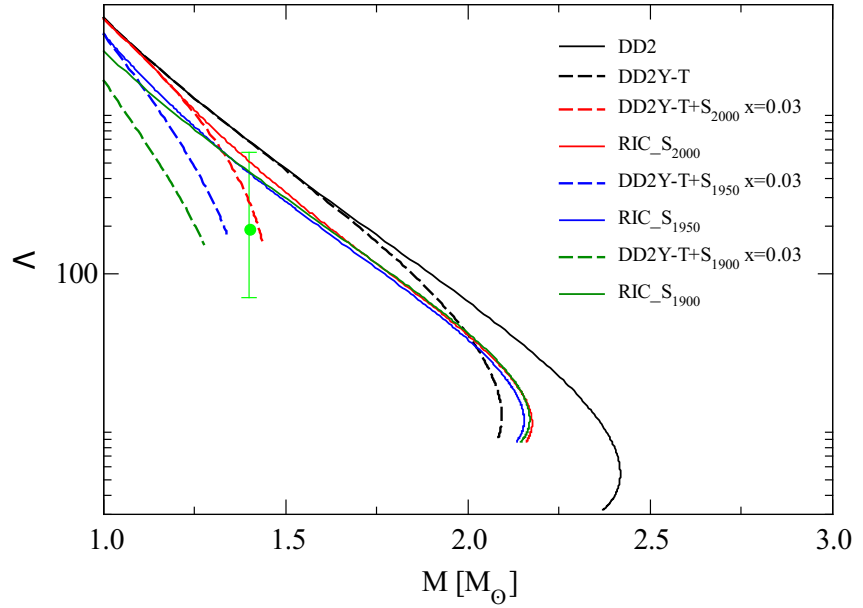


Figure 5. The dimensionless tidal deformability, denoted as Λ , is presented as a function of stellar mass for the ensemble of EoS illustrated in Figure 4. The green vertical line in the figure signifies the $\Lambda_{1.4}$ constraint derived from the low-spin prior analysis of GW170817, as reported in [9].

An intriguing outcome of DM production within the hadronic phase observed in Figure 5 is the fulfillment of the tidal deformability constraint. Without DM, both pure nucleonic EoS (DD2) and hyperonic EoS (DD2Y-T) fail to satisfy this constraint. However, the presence of S as a DM candidate plays a key role in softening the EoS around $1.4M_{\odot}$, ensuring that the tidal deformability constraint, as derived from the low-spin prior analysis of GW170817, is met for all hybrid EoS constructed by incorporating S into the hadronic EoS.

6. Conclusions

Inspired by the presence of a stable sexaquark configuration, denoted as $S=uuudds$, with a mass below 2054 MeV, a threshold ensuring a lifetime exceeding the age of the Universe [7], which renders it a compelling bosonic DM, we have undertaken an examination to determine if the maximum mass, radius, and tidal deformability measurements of NSs are consistent with the potential existence of this intriguing particle in the core of NS. We employed the generalized relativistic density functional model, as introduced in reference [36], to describe the hadronic phase, incorporating the presence of S particles as a bosonic DM. Our observations indicate that the incorporation of S in the hadronic phase, featuring a repulsive interaction with baryonic matter within the parameter range employed in this study, leads to a softening of the EoS. Consequently, this softening effect contributes to the correction of the tidal deformability problem exhibited by pure hadronic EoS. The superconducting quark matter phase was modeled using the nNJL model, as

outlined in reference [46], and we utilized a Replacement Interpolation Construction to develop a crossover phase transition between these two distinct phases. As a result, we modeled hybrid stars featuring a deconfined quark matter core surrounded by hypernuclear matter, including strange DM, all in accordance with the observational constraints of NSs. Our findings demonstrate that increasing the vacuum mass of the DM candidate is unfavorable to achieving the required softening of the EoS around $1.4M_{\odot}$ for satisfying the radius constraint of neutron stars. We have effectively constrained the upper limit of the sexaquark vacuum mass within our model to fall within the range of $1885 < m_S < 2000$ MeV, drawing upon the consistency of our previous findings presented in reference [36] with the outcomes of the present study. However, an increase in the effective mass of S with medium density is required to find stable neutron stars above the density threshold for the appearance of S. Within the scope of our analysis, we refrain from making a definitive assessment regarding the necessity of a sexaquark in explaining NS properties. Eventually, the cooling behavior of NSs could potentially yield indications of the presence of S particles as a viable candidate for DM within the NS core. Furthermore, it is important to underscore that the approach taken in this paper is wholly phenomenological.

Outlook: In our upcoming work, we intend to conduct a more comprehensive parameter scan for our dark matter candidate and carry out a more detailed investigation of its precise role in shaping the equation of state of neutron stars. This will allow us to further refine our understanding of its effects within NSs. Moreover, investigating the model-dependency of our results is also a goal of our future works.

Author Contributions: M.Sh. The idea, investigation, methodology, formal analysis and calculations, writing and preparing the original draft of the paper, D.R. checking consistency with the observational constraints, completing the draft, reviewing and editing, S.T. Obtaining and programming the hadronic matter EoS, reviewing and editing. All authors have read and agreed to the published version of the manuscript.

Funding: This research received no external funding

Institutional Review Board Statement: Not applicable

Data Availability Statement: Not applicable

Acknowledgments: M. Sh. has been supported by the program Excellence Initiative–Research University of the University of Wrocław of the Ministry of Education and Science. M. Sh. acknowledges the hospitality of the Frankfurt Institute for Advanced Studies (FIAS).

Conflicts of Interest: The authors declare no conflict of interest.

Abbreviations

The following abbreviations are used in this manuscript:

DM Dark Matter

EoS Equation of State

NSs Neutron Stars

WIMPs weakly interacting massive particles

GW gravitational-wave

NICER Neutron Star Interior Composition Explorer

S Sexaquark

QCD Quantum Chromodynamics

DD2 Parameterization of a GDRF for hadronic matter including only nucleons

DD2Y-T DD2 with hyperons by S. Typel

DD2Y-T+S DD2Y-T with sexaquark

GRDF Generalized relativistic density functional

MC Maxwell Construction

RIC Replacement Interpolation Construction

M-R Mass-Radius

References

1. I. de Martino, S. S. Chakrabarty, V. Cesare, A. Gallo, L. Ostorero and A. Diaferio, “Dark matters on the scale of galaxies,” *Universe* **2020** 6, 107.
2. P. Salucci, G. Esposito, G. Lambiase, E. Battista, M. Benetti, D. Bini, L. Boco, G. Sharma, V. Bozza and L. Buoninfante, *et al.* “Einstein, Planck and Vera Rubin: Relevant Encounters Between the Cosmological and the Quantum Worlds,” *Front. in Phys.* **2021** 8, 603190.
3. C. Kouvaris, *Phys. Rev. Lett.* **2012** 108, 191301.
4. G. Bertone and T. Tait, M.P., “A new era in the search for dark matter,” *Nature* **2018** 562, 51-56.
5. D. J. E. Marsh, “Axion Cosmology,” *Phys. Rept.* **2016** 643, 1-79.
6. A. V. Balatsky, B. Fraser and H. S. Røising, “Dark sound: Collective modes of the axionic dark matter condensate,” *Phys. Rev. D* **2022** 105, 023504.
7. G. R. Farrar, “A Stable Sexaquark: Overview and Discovery Strategies,” [arXiv:2201.01334 [hep-ph]].
8. M. Doser, G. Farrar and G. Kornakov, “Searching for a dark matter particle with anti-protonic atoms,” [arXiv:2302.00759 [hep-ph]].
9. B. P. Abbott *et al.* [LIGO Scientific and Virgo], “GW170817: Measurements of neutron star radii and equation of state,” *Phys. Rev. Lett.* **2018** 121, 161101. [arXiv:1805.11581 [gr-qc]].
10. M. C. Miller, F. K. Lamb, A. J. Dittmann, S. Bogdanov, Z. Arzoumanian, K. C. Gendreau, S. Guillot, A. K. Harding, W. C. G. Ho and J. M. Lattimer, *et al.* “PSR J0030+0451 Mass and Radius from NICER Data and Implications for the Properties of Neutron Star Matter,” *Astrophys. J. Lett.* **2019** 887, L24.
11. M. C. Miller, F. K. Lamb, A. J. Dittmann, S. Bogdanov, Z. Arzoumanian, K. C. Gendreau, S. Guillot, W. C. G. Ho, J. M. Lattimer and M. Loewenstein, *et al.* “The Radius of PSR J0740+6620 from NICER and XMM-Newton Data,” *Astrophys. J. Lett.* **2021** 918, L28.
12. T. E. Riley, A. L. Watts, S. Bogdanov, P. S. Ray, R. M. Ludlam, S. Guillot, Z. Arzoumanian, C. L. Baker, A. V. Bilous and D. Chakrabarty, *et al.* “A NICER View of PSR J0030+0451: Millisecond Pulsar Parameter Estimation,” *Astrophys. J. Lett.* **2019** 887, L21.
13. T. E. Riley, A. L. Watts, P. S. Ray, S. Bogdanov, S. Guillot, S. M. Morsink, A. V. Bilous, Z. Arzoumanian, D. Choudhury and J. S. Deneva, *et al.* “A NICER View of the Massive Pulsar PSR J0740+6620 Informed by Radio Timing and XMM-Newton Spectroscopy,” *Astrophys. J. Lett.* **2021** 918, L27.
14. E. Fonseca, H. T. Cromartie, T. T. Pennucci, P. S. Ray, A. Y. Kirichenko, S. M. Ransom, P. B. Demorest, I. H. Stairs, Z. Arzoumanian and L. Guillemot, *et al.* “Refined Mass and Geometric Measurements of the High-mass PSR J0740+6620,” *Astrophys. J. Lett.* **2021** 915, L12.
15. T. Dietrich, M. W. Coughlin, P. T. H. Pang, M. Bulla, J. Heinzel, L. Issa, I. Tews and S. Antier, “Multimessenger constraints on the neutron-star equation of state and the Hubble constant,” *Science* **2020** 370, 1450-1453.
16. D. R. Karkevandi, S. Shakeri, V. Sagun and O. Ivanytskyi, “Bosonic dark matter in neutron stars and its effect on gravitational wave signal,” *Phys. Rev. D* **2022** 105, 023001.
17. D. Rafiei Karkevandi, S. Shakeri, V. Sagun and O. Ivanytskyi, “Tidal deformability as a probe of dark matter in neutron stars,” doi:10.1142/9789811269776_0307.
18. S. Shakeri and D. R. Karkevandi, “Bosonic Dark Matter in Light of the NICER Precise Mass-Radius Measurements,” [arXiv:2210.17308 [astro-ph.HE]].
19. M. A. Perez-Garcia, J. Silk and J. R. Stone, “Dark matter, neutron stars and strange quark matter,” *Phys. Rev. Lett.* **2010** 105, 141101.
20. S. C. Leung, M. C. Chu and L. M. Lin, *Phys. Rev. D* **2011**, 84, 107301 doi:10.1103/PhysRevD.84.107301 [arXiv:1111.1787 [astro-ph.CO]].
21. A. Li, F. Huang and R. X. Xu, “Too massive neutron stars: The role of dark matter?” *Astropart. Phys.* **2012** 37, 70-74.
22. G. Panotopoulos and I. Lopes, *Phys. Rev. D* **2017**, 96, no.8, 083004 doi:10.1103/PhysRevD.96.083004 [arXiv:1709.06312 [hep-ph]].
23. J. Ellis, G. Hütsi, K. Kannike, L. Marzola, M. Raidal and V. Vaskonen, “Dark Matter Effects On Neutron Star Properties,” *Phys. Rev. D* **2018** 97, 123007.
24. A. Nelson, S. Reddy and D. Zhou, *JCAP* **2019**, 07, 012 doi:10.1088/1475-7516/2019/07/012 [arXiv:1803.03266 [hep-ph]].
25. O. Ivanytskyi, V. Sagun and I. Lopes, “Neutron stars: New constraints on asymmetric dark matter,” *Phys. Rev. D* **2020** 102, 063028.
26. V. Sagun, E. Giangrandi, O. Ivanytskyi, I. Lopes and K. A. Bugaev, “Constraints on the fermionic dark matter from observations of neutron stars,” *PoS PANIC2021* **2022**, 313.
27. H. M. Liu, J. B. Wei, Z. H. Li, G. F. Burgio and H. J. Schulze, “Dark matter effects on the properties of neutron stars: Optical radii,” *Phys. Dark Univ.* **2023** 42, 101338.
28. V. Parmar, H. C. Das, M. K. Sharma and S. K. Patra, “Influence of dark matter on magnetized neutron stars,” *Phys. Rev. D* **2023** 108, 083003.

29. P. Thakur and T. K. Jha, "Neutron stars with fermionic dark matter: a two fluid approach," *DAE Symp. Nucl. Phys.* **2023** 66, 776-777.
30. M. ShahrbaF, "Appearance of sexaquark in the core of neutron stars as a candidate of dark matter," *J. Phys. Conf. Ser.* **2023** 2536, 012001.
31. N. Rutherford, G. Raaijmakers, C. Prescod-Weinstein and A. Watts, "Constraining bosonic asymmetric dark matter with neutron star mass-radius measurements," *Phys. Rev. D* **2023**, 107, 103051.
32. S. Shirke, S. Ghosh, D. Chatterjee, L. Sagunski and J. Schaffner-Bielich, "R-modes as a New Probe of Dark Matter in Neutron Stars," [arXiv:2305.05664 [astro-ph.HE]].
33. H. R. Rüter, V. Sagun, W. Tichy and T. Dietrich, "Quasi-equilibrium configurations of binary systems of dark matter admixed neutron stars," [arXiv:2301.03568 [gr-qc]].
34. G. R. Farrar, "A stable H dibaryon: Dark matter candidate within QCD?" *Int. J. Theor. Phys.* **2003** 42, 1211-1218.
35. R. L. Jaffe, "Perhaps a Stable Dihyperon," *Phys. Rev. Lett.* **1977** 38, 195-198 [erratum: *Phys. Rev. Lett.* **38** (1977), 617]
36. M. ShahrbaF, D. Blaschke, S. Typel, G. R. Farrar and D. E. Alvarez-Castillo, "Sexaquark dilemma in neutron stars and its solution by quark deconfinement," *Phys. Rev. D* **2022** 105, 103005.
37. S. Typel and H. H. Wolter, "Relativistic mean field calculations with density dependent meson nucleon coupling," *Nucl. Phys. A* **1999** 656, 331-364.
38. S. Typel, "Relativistic model for nuclear matter and atomic nuclei with momentum-dependent self-energies," *Phys. Rev. C* **2005** 71, 064301.
39. S. Typel, G. Ropke, T. Klahn, D. Blaschke and H. H. Wolter, "Composition and thermodynamics of nuclear matter with light clusters," *Phys. Rev. C* **2010** 81, 015803.
40. J. R. Stone, V. Dexheimer, P. A. M. Guichon, A. W. Thomas and S. Typel, "Equation of state of hot dense hyperonic matter in the Quark-Meson-Coupling (QMC-A) model," *Mon. Not. Roy. Astron. Soc.* **2021** 502 no.3, 3476-3490.
41. M. ShahrbaF and H. R. Moshfegh, "Appearance of hyperons in neutron stars within LOCV method," *Annals Phys.* **2019** 402, 66-77.
42. M. ShahrbaF, D. Blaschke, A. G. Grunfeld and H. R. Moshfegh, "First-order phase transition from hypernuclear matter to deconfined quark matter obeying new constraints from compact star observations," *Phys. Rev. C* **2020** 101, 025807.
43. M. ShahrbaF, H. R. Moshfegh and M. Modarres, "Equation of state and correlation functions of hypernuclear matter within the lowest order constrained variational method," *Phys. Rev. C* **2019** 100, 044314.
44. M. ShahrbaF, D. Blaschke and S. Khanmohamadi, "Mixed phase transition from hypernuclear matter to deconfined quark matter fulfilling mass-radius constraints of neutron stars," *J. Phys. G* **2020** 47, 115201.
45. A. E. Radzhabov, D. Blaschke, M. Buballa and M. K. Volkov, "Nonlocal PNJL model beyond mean field and the QCD phase transition," *Phys. Rev. D* **2011** 83, 116004.
46. M. ShahrbaF, S. Antić, A. Ayriyan, D. Blaschke and A. G. Grunfeld, "Constraining free parameters of a color superconducting nonlocal Nambu-Jona-Lasinio model using Bayesian analysis of neutron stars mass and radius measurements," *Phys. Rev. D* **2023** 107, 054011.
47. B. P. Abbott *et al.* [LIGO Scientific and Virgo], "GW170817: Observation of Gravitational Waves from a Binary Neutron Star Inspiral," *Phys. Rev. Lett.* **2017**, 119, 161101.
48. B. P. Abbott *et al.* [LIGO Scientific and Virgo], "GW190425: Observation of a Compact Binary Coalescence with Total Mass $\sim 3.4M_{\odot}$," *Astrophys. J. Lett.* **2020**, 892, L3.
49. T. Hinderer, "Tidal Love numbers of neutron stars," *Astrophys. J.* **2008**, 677, 1216-1220.
50. T. Hinderer, B. D. Lackey, R. N. Lang and J. S. Read, "Tidal deformability of neutron stars with realistic equations of state and their gravitational wave signatures in binary inspiral," *Phys. Rev. D* **2010**, 81, 123016.

Disclaimer/Publisher's Note: The statements, opinions and data contained in all publications are solely those of the individual author(s) and contributor(s) and not of MDPI and/or the editor(s). MDPI and/or the editor(s) disclaim responsibility for any injury to people or property resulting from any ideas, methods, instructions or products referred to in the content.